2021 5th Scientific School Dynamics of Complex Networks and their Applications (DCNA) | 978-1-6654-4283-1/21/$31.00 ©2021 IEEE | DOI: 10.1109/DCNA53427.2021.9586890

Factor of border crossing limitation with an infection hub in the SIR covid model

Vladimir Khorev
Center for technologies in robotics and mechatronics components
Innopolis University
Innopolis, Russia
Orcid: 0000-0001-6613-8940

Victor B. Kazantsev
Neurotechnology deparment
Lobachevsky University
Nizhniy Novgorod, Russia
Center for technologies in robotics and mechatronics components
Innopolis University
Innopolis, Russia
Center for Neurotechnology and Machine Learning
Immanuel Kant Baltic Federal University
Kaliningrad, Russia
Orcid: 0000-0002-2881-6648

***Abstract*—In this work we develop a new nonlinear net-based SIR epidemic problem modeling the spreading of coronavirus under the effect of a border crossing limits by the government measures to stop coronavirus spreading. We show that the emergence and disappearance of subsequent waves of infection on the degree of relationship with a hub is non-linear, and with a large degree of relationships, the number of waves can decrease.**

***Index Terms*—COVID-19; forecasting; nonlinear SIR model; border closing**

I. Introduction

The SARS-COV-2 coronavirus pandemic is currently increasing the interest of researchers to SIR models [1] and many works for different regions of the world [2]–[6] demonstrate their satisfactory performance, although there are other points of view [7]. Nevertheless, the question of the influence of quarantine on the flow of infection is still require further research [8]–[10]. There are many examples of network approach application to analysis of social, ecological and biological systems [8], [11]–[15]. Given the success demonstrated by the examples of using a network approach to model social systems, we decided to upgrade existing models in this way.

II. Model

For k interacting elements, in general, the system of differential equations will look like this:

$$\begin{aligned}
&\dot{S}_i = -\beta \sum_j p_j S_i + \delta R_i - dH_i S_i + \mu_i \ (i,j = 1..k);\\
&\dot{I}_i = \beta \sum_j p_j S_i + dH_i S_i - (\gamma + \varepsilon) I_i;\\
&\dot{R}_i = \gamma I_i - \delta R_i;\\
&\dot{H}_i = \alpha I_i - bH_i;
\end{aligned} \tag{1}$$

This work is supported by Russian Foundation for Basic Research (grant 20-04-60078).

Here, $S_i(t)$ denotes the number of susceptible individuals of the i-th region, $I(t)$ — infected, $R(t)$ — recovered, $H(t)$ non-human carriers (viruses). The coefficient α denotes the number of carriers (viruses) emitted by an infected individual, β is the probability of infection in the case of contact of a susceptible subject with an infected subject, γ is the probability of recovery (usually, it is interpreted as the rate of recovery, since the average duration of the subject is in the state of infection is $1/\gamma$), δ is the probability of losing immunity and the appearance of the possibility of re-infection, ε is the probability of death, μ_i — the immigration of the population for the i-th region, p_j is the interaction coefficient between the j-th and i-th districts given from the communication matrix (P), Relative degree of openness of the borders, which is relevant for modeling quarantine events [16], b denotes the coefficient of natural loss of carriers, d is the degree of contagiousness of the carrier (virulence). It should be noted that in the case of $p = 0$ (complete closure of boundaries), the system is degenerated in case of infecting one subject in the absence of the remaining infection [17]. To check the effect of the presence of the central district (Hub), as well as the observed difference between the second and third areas, the communication matrix was as follows:

$$P = \begin{bmatrix} 1 & p & p \\ p & 0.5 & 0.05 \\ p & 0.05 & 0.1 \end{bmatrix} \tag{2}$$

III. Results

The second and third districts are located in the outskirts and have weak interaction between themselves. The first area is considered as a hub, and the its level of exposure to other districts can vary. Typical curves for a small bond ($p = 0.1$) are shown in Fig. 1. The numerical simulation showed that despite the fact that the probability of internal infection in the third area is five times lower than in the second, the final number of infected differs by about twice. The graphs of the total infected over time for the degree of opening

978-1-6654-4283-1/21/$31.00 ©2021 IEEE

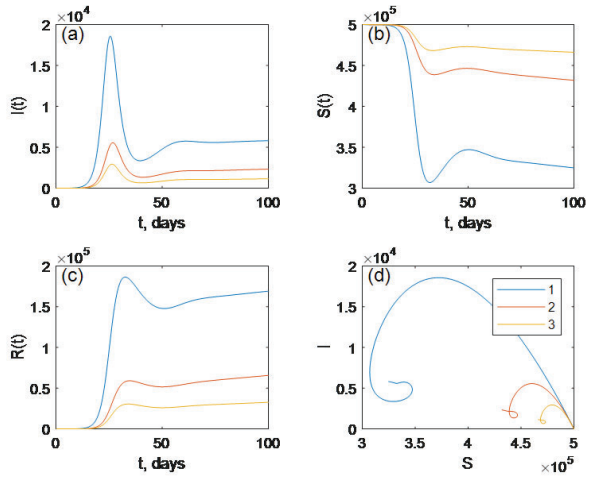

Fig. 1. The time series of infected (a), susceptible (b) and recovered (c), as well as the phase portrait for three districts (d), obtained for the values of the system parameters with the communication matrix 2: $n = 50000$, $\beta = 1.9$, $\gamma = 1.5$, $\delta = 0.05$, $b = 0.01$, $d = 10^{-7}$, $p = 0.1$.

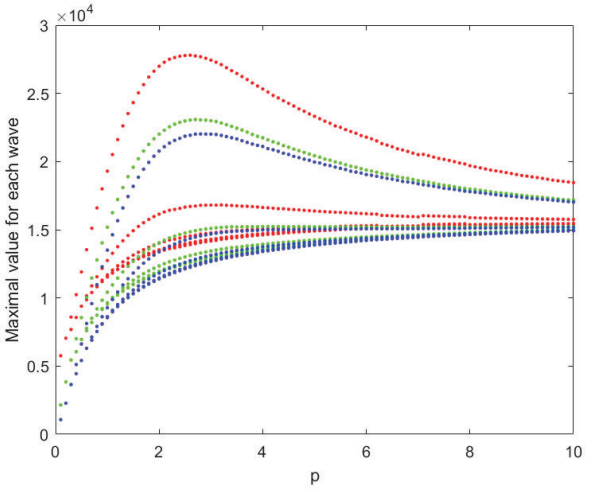

Fig. 2. The dependence of the maximum number of infected in the second and subsequent waves in areas (red – 1, green – 2, blue – 3) on the degree of openness of the boundaries between the hub and other districts (p).

of the borders for the districts are similar to the dynamics with the case of symmetric links, despite the difference in the probability of infection inside the areas and are primarily determined by the degree of relationship with a hub, which can be seen for the first wave, but the flow and final values of infected dependent from the internal probabilities of infection with small communication values a hub. The final amount of infected in the area increases with a degree of connection with a hub. However, this dependence is close to a logarithmic form, and the maximum value (peak of the wave) number of infectios demonstrates almost linear growth for the communication values with a hub of more than 0.5. Despite the difference in the likelihood of infection within the districts, infection curves are primarily determined by the degree of relationship with a hub, which can be seen for the first wave, but the flow and final values of infected depend on the internal probabilities of infection with small connections with a hub. The occurrence and disappearance of subsequent waves of infection on the degree of relationship with a hub is non-linear, and with a large extent relationship the number of waves even decreases, and their amplitude is committed to a constant value as shown in Fig. 2.

IV. Conclusion

Thus we developed a new nonlinear net-based SIR epidemic problem modeling the spreading of coronavirus under the effect of a border crossing limits by the government measures to stop coronavirus spreading. We show that the emergence and disappearance of subsequent waves of infection on the degree of relationship with a hub is non-linear, and with a large degree of relationships, the number of waves can decrease.

References

[1] Kermack, W. O., McKendrick , A. G. A Contribution to the Mathematical Theory of Epidemics. Proc. Roy. Soc. Lond. 115, pp. 700–721 (1927).

[2] Gounane, S., et al. An adaptive social distancing SIR model for COVID-19 disease spreading and forecasting. Epidemiologic Methods. 10 (2021).

[3] Giordano, G., et al. Modelling the COVID-19 epidemic and implementation of population-wide interventions in Italy. Nat Med 26, pp. 855–860 (2020).

[4] Abou-Ismail, A. Compartmental Models of the COVID-19 Pandemic for Physicians and Physician-Scientists. SN Compr. Clin. Med. 2, pp. 852–858 (2020).

[5] Fokas, A. S., Dikaios, N., Kastis, G. A. Mathematical models and deep learning for predicting the number of individuals reported to be infected with SARSCoV-2. J. R. Soc. Interface 17, 20200494 (2020).

[6] Deldar, M., Tahmasebi-Ghorabi, S., Sayehmiri, K. SIR Model for Estimations of the Coronavirus Epidemic Dynamics in Iran. 6(2), pp. 101–106 (2020).

[7] Moein, S., Nickaeen, N., Roointan, A. Inefficiency of SIR models in forecasting COVID-19 epidemic: a case study of Isfahan. Sci Rep 11, 4725 (2021).

[8] Estrada E. COVID-19 and SARS-CoV-2. Modeling the present, looking at the future. Phys Rep. 869, 1–51 (2020).

[9] Boccaletti, S., Mindlin, G., Ditto, W., Atangana, A. Closing editorial: Forecasting of epidemic spreading: lessons learned from the current covid-19 pandemic. Chaos, Solitons and Fractals, 139 (2020).

[10] Boccaletti, S., Ditto, W., Mindlin, G., Atangana, A. Modeling and forecasting of epidemic spreading: The case of Covid-19 and beyond. Chaos, Solitons and Fractals, 135 (2020).

[11] Makarov V.V., et al. Emergence of a multilayer structure in adaptive networks of phase oscillators. Chaos, Solitons and Fractals. 84, pp. 23–30 (2016).

[12] Makarov V.V., et al. Assortative mixing in spatially extended networks. Sci.Rep. 8, 13825 (2018).

[13] Hramov A. E., et al. Functional networks of the brain: from connectivity restoration to dynamic integration. Phys. Usp. 64(6) (2021).

[14] Pitsik E.N., et al. Inter-layer competition in adaptive multiplex network. New Journal of Physics. 20, 075004 (2018).

[15] Kurkin, S.A., Hramov, A. E., Chholak, P., Pisarchik, A. Localizing oscillatory sources in a brain by meg data during cognitive activity. 4th International Conference on Computational Intelligence and Networks (CINE), pp. 1–4 (2020).

[16] Wood J. G., Mccaw J., Becker N. G., Nolan T., MacIntyre C. R., Optimal dosing and dynamic distribution of vaccines in an influenza pandemic, American Journal of Epidemiology, 169, pp. 1517–1524 (2009).

[17] Tien, J. H., Earn, D. J. D. Multiple Transmission Pathways and Disease Dynamics in a Waterborne Pathogen Model. Bulletin of Mathematical Biology, 72(6), pp. 1506–1533 (2010).